http://dx.doi.org/10.5935/0103-5053.20160197
J. Braz. Chem. Soc., Vol. 28, No. 4, 557-566, 2017.
Printed in Brazil - ©2017 Sociedade Brasileira de Química
0103 - 5053 $6.00+0.00

Article

Anodic Oxidation of Sulfide to Sulfate: Effect of the Current Density on the Process Kinetics

Paulo C. Caliari,[,a,b] Maria J. Pacheco,[a] Lurdes F. Ciríaco[a] and Ana M. C. Lopes[a]*

[a]*FibEnTech-UBI and Department of Chemistry, Universidade da Beira Interior, 6201-001 Covilhã, Portugal*

[b]*Instituto Federal de Educação, Ciência e Tecnologia do Espírito Santo, 29106-210 Vila Velha-ES, Brazil*

The kinetics of the conversion of sulfide to sulfate by electro-oxidation, using a boron-doped diamond (BDD) electrode was studied. Different applied current densities were tested, from 10 to 60 mA cm^{-2}. The results showed that the electrochemical conversion of sulfide to sulfate occurs in steps, via intermediate production of other sulfur species. The oxidation rate of the sulfide ion is dependent on its concentration and current density. The reaction order varies with the current intensity, being 2 for the lower applied current intensity and high S^{2-} concentration, which is compatible with a mechanism involving two S^{2-} ions to give S_2^{2-}. For higher current densities, where current control is less important, reaction order varies from 0.15 to 0.44 for the current densities of 20 and 60 mA cm^{-2}, respectively. For the formation of SO_4^{2-} from S^{2-} electro-oxidation, the reaction orders with respect to sulfide concentration and current intensity are 0 and 1, respectively.

Keywords: sulfide oxidation, sulfate formation, electrochemical oxidation, BDD, kinetic study

Introduction

Sulfide ion is toxic, odorous and corrosive and is of particular concern in sewer systems, since it causes pipes corrosion.[1,2] The presence of S^{2-} in sewage systems is a common problem due to the stimulation of the metabolic activity of sulfate-reducing bacteria, given the high organic load and low dissolved oxygen.[3] Sulfide is one of the contaminants in effluents generated in the extraction of oil and gas and in certain types of wastes from oil refinery,[4] as well as in wastewaters from the leather industry that present high concentration in sulfide ion.[5] Concrete corrosion problems have also been reported for S^{2-} concentration between 0.1 and 0.5 mg L^{-1}.[6]

A variety of physicochemical methods, like chemical oxidation and catalytic conversion, have been used to oxidize S^{2-} to elemental sulfur or sulfate, thus achieving its removal from the wastewater.[7] In the past, the removal of S^{2-} from effluents was performed by precipitation, as ZnS, and by oxidation with chromate in alkaline media.[8] However, these treatments are expensive, due to the added chemicals, and environmentally incompatible, because of the disposal of the resulting toxic sludge. The biological oxidation to remove S^{2-} can also be performed, but it is slow and applies only to low S^{2-} concentrations.[4]

The electrochemical processes are a promising technique for the resolution of pollution problems, since they present (*i*) versatility: direct or indirect oxidation, phase separation, biocides functions, treatment of many different contaminants; and (*ii*) energetic efficiency: electrochemical processes generally have lower temperature requirements, the potential can be controlled and electrodes and cells can be designed to minimize energy losses due to voltage drops, poor current distribution and secondary reactions.[9] In the recent years, there has been a growing interest in these processes for the treatment of wastewaters containing recalcitrant and biotoxic compounds.[10] The electrochemical treatment also offers an environmentally attractive method to remove S^{2-} ions, since the anodic oxidation of this species produces less toxic products.[11]

Sulfide is an electrochemically active component that can react at the anode and directly donate electrons to the electrode.[7] Thus, it can be removed from the aqueous solution without the production of sludge, by oxidation to elemental sulfur or oxyanions, like SO_4^{2-}, which are ecologically benign.[8] According to the potential diagrams

*e-mail: caliari@outlook.com

vs. pH for the various species involved in the oxidation of S^{2-} solutions[12-14] and, depending on the experimental conditions, during the S^{2-} oxidation several sulfur intermediate species, such as polysulfides (S_x^{2-}, with x = 2, 3, 4, ...), dithionite, sulfite, tetrathionate, and thiosulfate, can be formed.[7,15-18]

Ateya and Al-Kharafi[19] studied the electrochemical oxidation of sulfide solutions, with concentrations between 0.001 and 0.005 mol L^{-1}, using NaCl as supporting electrolyte, and observed sulfur deposition on the surface of the graphite anode, a fact that was also observed later.[11] According to these authors, the continuous oxidation to sulfur oxyanions should be much slower than the oxidation of S^{2-} to sulfur. The formation of elemental sulfur as an intermediate in the anodic oxidation of S^{2-} process was also evidenced in another study[20] that assigned the oscillations in the voltammograms of the S^{2-} electro-oxidation, at a Ti/Ta_2O_5-IrO_2 anode, to the continuous formation and removals of sulfur on the electrode's surface. Likewise, during the anodic oxidation of S^{2-} in real and simulated wastewaters, using as anode titanium coated with Ir/Ta oxides, the formation of elemental sulfur was also observed.[21] However, the deposition of elemental sulfur, which may lead to the electrode's surface passivation, was not observed in the anodic oxidation of S^{2-}, present in a domestic wastewater, using as anodes titanium coated with different metal oxide (TaO_2/IrO_2: 0.35/0.65), (RuO_2/IrO_2: 0.70/0.30), (PtO_2/IrO_2: 0.70/0.30), SnO_2 or PbO_2.[22] However, in this study, S^{2-} concentration was 10 mg L^{-1} and in the previous case[21] ranged between 30 and 90 mg L^{-1}. Thus, the formation and deposition of sulfur seems to be influenced by the S^{2-} concentration. The electrochemical oxidation of S^{2-} was also performed by Waterston *et al*.,[8] using a boron-doped diamond (BDD) anode, and it was found that its conversion to SO_4^{2-} occurred almost quantitatively with a current efficiency of 90%. This situation seems to show the best performance of this electrode material, BDD, when compared to others. In fact, the efficacy of the electrochemical oxidation depends strongly on the electrode materials. According to Panizza and Cerisola,[23] complete oxidation and good energetic efficiency can only be obtained at high oxygen overpotential anodes, such as boron-doped diamond, BDD. This electrode material presents great features, namely, higher chemical inertness, greater current efficiencies, longer lifetime and higher overpotential for oxygen evolution than that of other conventional anodes. It also enables the production of large amounts of weakly adsorbed $^{\bullet}OH$, which leads to an efficient oxidation of the pollutants, at the anode's surface or in its vicinity.[23,24]

The electrochemical oxidation of S^{2-} can be achieved by direct oxidation, at the electrode surface, or by indirect oxidation, through oxidizing agents like $^{\bullet}OH$, O_2 and chlorine active species generated at the anode surface.[21] The oxidation can be controlled by mass transfer or by electrons transfer, from the sulfide ion to the surface of the anode.[19] Thus, the removal of S^{2-} via electro-oxidation may show different trends regarding the experimental conditions. Zero-order kinetics (kinetic control) was observed in the presence and in the absence of NaCl during the oxidation of S^{2-} at BDD.[8] These results are significantly different from those obtained in the oxidation of S^{2-} using a Ti/IrO_2-Ta_2O_5 anode, with kinetic orders ranging from 0.5 and 0.9.[4] The feasibility of S^{2-} electro-oxidation was also observed in the electrolysis of a tannery wastewater with Ti/MO (MO = metal oxide) anodes, without, however, being identified the formed intermediates.[25]

Despite the studies found in the literature describing the S^{2-} anodic electro-oxidation, only a few are focused on the electro-oxidation of sulfide to sulfate.[8] Also, in these few studies low sulfide concentration was used, with low assay duration and small range of applied current density. This situation limits the understanding of the kinetics of the conversion sulfide/sulfate. Thus, the objective of this study was to evaluate the effect of the current density on the kinetics of the conversion of sulfide into sulfate, by anodic oxidation at a BDD electrode, using high sulfide concentration.

Experimental

Chemicals

The following analytical grade reagents were used without further purification: hydrated sodium sulfide, $Na_2S.9H_2O$, 99.4%, Merck; hydrochloric acid, HCl, 37%, Sigma-Aldrich; sulfuric acid, H_2SO_4, 98%, VWR Chemicals; sodium hydroxide, NaOH, 98%, Panreac Chemical UAA; soluble starch, ACS, Riedel-de Haen; penta-hydrate sodium thiosulfate, $Na_2S_2O_3.5H_2O$, 99.5%, Merck; potassium hydrogen biodate, $KH(IO_3)_2$, ACS, 99.8%, Merck; potassium iodide, KI, 99%, ACS, Carlo Erba; iodine, I_2, ACS, 99.8%, Riedel-de Haen.

Electrochemical characterization of sulfide solutions

Sulfide aqueous solutions, 60 mmol L^{-1}, were characterized by cyclic voltammetry, in a one-compartment three electrode cell, utilizing as working electrode a BDD electrode, purchased from Adamant Technologies, now NeoCoat (0.15 cm^2 working area), as counter electrode a platinum plate (1 cm^2) and as reference electrode a commercial saturated Ag/AgCl, KCl_{sat} electrode. The voltammograms were recorded using a potentiostat/

galvanostat VoltaLab PGZ 301 at scan rates of 10, 100, and 1000 mV s^{-1}.

Electrodegradation assays

Electrochemical experiments were performed in an one-compartment cell, working in batch mode with stirring, with a 10 cm^2 BDD electrode (purchased from Adamant Technologies, now NeoCoat) as the anode and a 10 cm^2 stainless steel plate as the cathode, with a 1 cm inter-electrodes gap. Current densities varied from 10 to 60 mA cm^{-2} and were imposed by a power supply unit, Laboratory DC Power Supply, Model GPS-3030D (0-30 V, 0-3 A). Stirring was accomplished by a magnetic stirrer, Metrohm AG.

The Na_2S solutions, 500 mL, with S^{2-} concentration of 1953 ± 49 mg L^{-1} (approximately 60 mmol L^{-1}) were electrolyzed in an open system, during the proposed experimental periods. The run time was 42 h for the applied current densities of 10 mA cm^{-2}, 20 h for 20, 30 and 40 mA cm^{-2}, 17 h for 50 mA cm^{-2}, and 15 h for 60 mA cm^{-2}. Samples were collected hourly for analyzes. The determination of S^{2-} concentration was performed according to APHA,[26] method 4500-S^{2-}. The presence of sulfur on the surface of BDD was investigated by scanning electron microscopy and energy dispersive X-ray spectroscopy analysis (SEM/EDS), performed in a Hitachi (S-3400N)/Oxford (60-74) system operating at 20 keV. The concentration of SO_4^{2-} was determined by ion chromatography, using a Shimadzu 20A Prominence HPLC system that was equipped with a conductivity detector CDD 10Avp. An IC I-524A Shodex (4.6 mm i.d. × 100 mm) column was employed. The mobile phase consisted of a 2.5 mmol L^{-1} phthalic acid aqueous solution with 2.3 mmol L^{-1} of tris(hydroxymethyl) aminomethane, at a flow rate of 1.5 mL min^{-1}. The column temperature was 40 °C. All solutions for the chromatographic analysis were prepared with ultrapure water obtained with Milli-Q® equipment. Electrical conductivity was measured with a Mettler Toledo conductivity meter, SevenEasy S30K, and pH with a Hanna pH meter, HI 931400.

Results and Discussion

Sulfur and polysulfides: production and features

Figure 1 presents a cyclic voltammogram run with a 60 mmol L^{-1} sulfide aqueous solution at a scan rate of 100 mV s^{-1}. Several peaks can be observed, analogous to what had already been observed by Al-Kharafi *et al.*[27] with a Pt working electrode. These authors have observed 3 consecutive peaks at –0.1, 0.475 and 1.0 V, which were assigned, respectively, to the following electrode processes: hydrogen sulfide oxidation to sulfur, followed by the partial formation of polysulfide species, which are oxidized to sulfate at higher potentials. Thus, when BDD is the working electrode, the 3 peaks observed in the oxidation curve of the voltammogram presented in the Figure 1 can be assigned to the next processes: sulfide oxidation to sulfur, at BDD surface (equation 1); formation of different polysulfide species (equation 2); and oxidation of the polysulfide species to sulfate (equation 3) that happens only at higher potentials, reached only for higher applied current densities.

$$BDD + S^{2-} \rightarrow (BDD)S + 2e^- \quad (1)$$

$$(BDD)S + S_x^{2-} \rightarrow BDD + S_{x+1}^{2-} \quad (2)$$

$$(BDD)S + 8OH^- \rightarrow BDD + 4H_2O + SO_4^{2-} + 6e^- \quad (3)$$

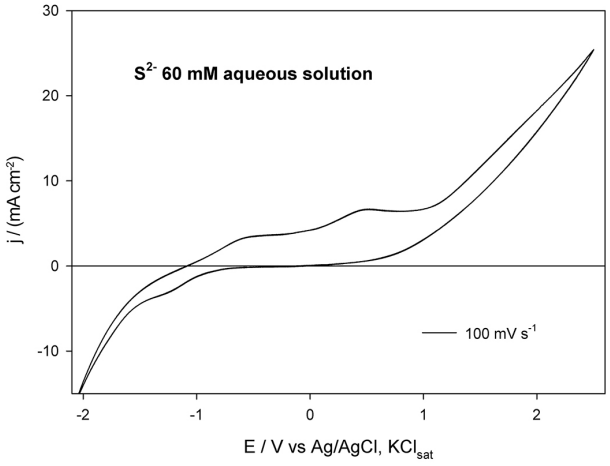

Figure 1. Cyclic voltammogram for the system BDD (0.15 cm^2) / S^{2-} (60 mmol L^{-1}) at a scan rate of 100 mV s^{-1}.

The formation of sulfur on the surface of the BDD anode was confirmed by SEM/EDS analysis (data not shown) and was due to the occurrence of equation 1.[14,27] The extent of this reaction was directly associated to the current intensities utilized, i.e., the formation of sulfur on the surface of the anode increased with the applied current density from 10 to 60 mA cm^{-2}.

During the assays performed at 10, 20 and 30 mA cm^{-2} no significant variation of the potential was observed, whereas for the assays performed at 40, 50 and 60 mA cm^{-2} the potential decreased in the beginning of the assays and slightly increased after some time, as can be seen in Figure 2a.

For higher current densities, the initial decrease in the potential must be related to an increase in the formation rate of sulfate rather than sulfur, which would also be responsible for a partial passivation of the electrode's surface. This passivation may explain the slight increase

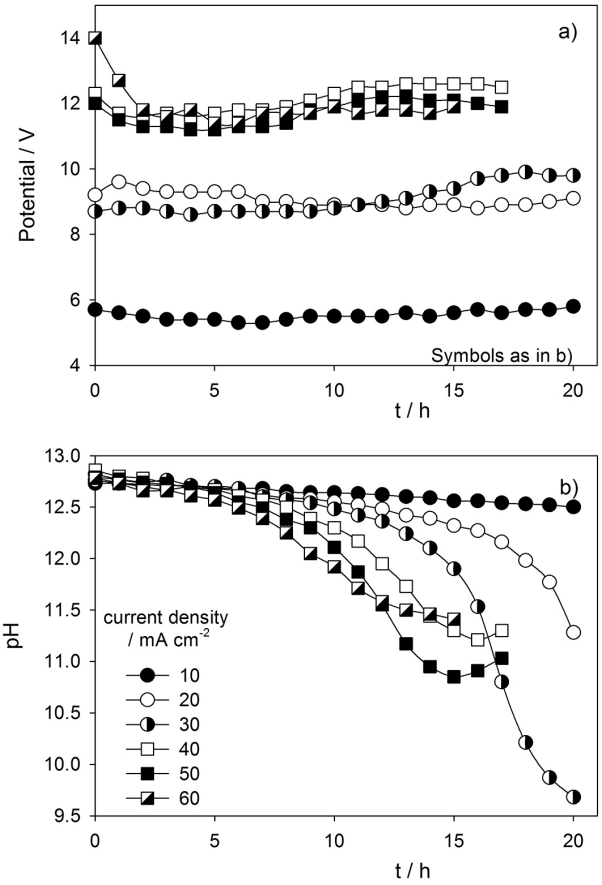

Figure 2. (a) Variation of potential difference between anode and cathode with time and (b) variation of pH with time for the assays performed at different applied current densities. $[S^{2-}]_0$ = 60 mmol L^{-1}.

in the potential at 20 and 30 mA cm^{-2} at the beginning of the assays, since at low current densities reactions involving less electrons transfer become more important (equation 1). Similar results were also obtained by other authors.[4,7,8,11,14,19,20,27,28] However, at low current density, 10 mA cm^{-2}, and low S^{2-} concentration, 10 mg L^{-1}, the presence of elemental sulfur was not observed.[22]

In this study, besides the formation of sulfur on the anode's surface, it was also observed the development of a yellow color in the solution. According to the literature,[4,8,11,17,27] this phenomenon was related with the formation of polysulfides, S_x^{2-}. The formed sulfur can react with S_x^{2-} to form S_{x+1}^{2-} (equation 2),[14,27] which can be further oxidized (equations 4-6),[12] resulting in a color intensification.[11]

$$3S_2^{2-} \rightarrow 2S_3^{2-} + 2\,e^- \quad (4)$$
$$4S_3^{2-} \rightarrow 3S_4^{2-} + 2\,e^- \quad (5)$$
$$5S_4^{2-} \rightarrow 4S_5^{2-} + 2\,e^- \quad (6)$$

Regarding pH variation during the assays performed at different applied current density (Figure 2b), all initial solutions presented pH values between 12.7 and 12.9, which decreased during the experiment. The results showed that the pH decay appeared to be directly related to the applied current density, particularly during the first 10 hours of the experiments.

The decrease in pH is associated with the occurrence of several possible reactions, such as those shown in equations 3 and 7 to 10, since the S^{2-} consumption is accompanied by OH^- consumption.[14]

$$4S^{2-} + 12OH^- \rightarrow S_4O_6^{2-} + 6H_2O + 18e^- \quad (7)$$
$$S^{2-} + 6OH^- \rightarrow SO_3^{2-} + 3H_2O + 6e^- \quad (8)$$
$$2S^{2-} + 6OH^- \rightarrow S_2O_3^{2-} + 3H_2O + 8e^- \quad (9)$$
$$S^{2-} + 8OH^- \rightarrow SO_4^{2-} + 4H_2O + 8e^- \quad (10)$$

The intermediate species, eventually formed, may be involved in further reactions, equations 11 to 13,[14] which can contribute to the consumption of OH^-, thus lowering also the pH.

$$S_2O_3^{2-} + 10OH^- \rightarrow 2SO_4^{2-} + 5H_2O + 8e^- \quad (11)$$
$$S_4O_6^{2-} + 20OH^- \rightarrow 4SO_4^{2-} + 10H_2O + 14e^- \quad (12)$$
$$SO_3^{2-} + 2OH^- \rightarrow SO_4^{2-} + H_2O + 2e^- \quad (13)$$

Another possible scenario is associated with equations 14 to 16, where H^+ is a product, with the consequent decrease in pH.[12] Also, all the reactions that lead to a decrease in the S^{2-} concentration induce the displacement of equation 17 to produce S^{2-} with OH^- consumption, intensifying the decrease in pH.[29]

$$2S^{2-} + 3H_2O \rightarrow S_2O_3^{2-} + 6H^+ + 8e^- \quad (14)$$
$$S^{2-} + 3H_2O \rightarrow SO_3^{2-} + 6H^+ + 6e^- \quad (15)$$
$$S^{2-} + 4H_2O \rightarrow SO_4^{2-} + 8H^+ + 8e^- \quad (16)$$
$$HS^- + OH^- \leftrightarrows S^{2-} + H_2O \quad (17)$$

After 10 hours for the assay performed at an applied current density of 60 mA cm^{-2}, 15 h for 50 mA cm^{-2}, and 16 h for 40 mA cm^{-2}, i.e., when S^{2-} concentration was already very low, it was observed a slight increase in the pH (Figure 2b). This situation may result from the reduction at the cathode of some intermediate species generated during the process (equations 18 and 19).[30]

$$2SO_3^{2-} + 3H_2O + 4e^- \rightarrow S_2O_3^{2-} + 6OH^- \quad (18)$$
$$2SO_3^{2-} + 2H_2O + 2e^- \rightarrow S_2O_4^{2-} + 4OH^- \quad (19)$$

Sulfide removal: effect of current density and kinetic aspects

Regarding the sulfide removal, the results showed that it is strongly influenced by the applied current density

(Figure 3a). The efficiency of the electro-oxidation process, expressed as sulfide removal *versus* electrical charge passed, at the different applied current densities, is depicted in Figure 3b, showing a decrease in efficiency with the increase in applied current due to an increase in the relevance of the diffusional step. After 8 h of electrolysis, sulfide removals were 34.3, 84.8, 97.8, 99.8, 99.2 and 99.4% for the applied current densities of 10, 20, 30, 40, 50 and 60 mA cm^{-2}, respectively. However, if it is considered the time needed to remove 50% of the initial S^{2-} (inset of Figure 3b), the results showed that increasing current density does not decrease substantially the time needed to achieve the desired removal, particularly for current densities between 40 and 60 mA cm^{-2}, since for these current densities the time decreases from 6.2 to 4.9 h. Nevertheless, when the density increases from 10 to 40 mA cm^{-2}, the time to achieve 50% removal in $[S^{2-}]$ is reduced from 29.8 to 6.2 h. The influence of the current density on the S^{2-} consumption is shown by the occurrence of, for instance, equations 1 and 7 to 10, since the increase in current density tends to enhance the occurrence of these reactions, having also influence on their relative occurrence.

Kinetic models based on kinetic control (i.e., current control, with reaction rate independent of S^{2-} concentration) and diffusion control (reaction rate dependent on S^{2-} concentration) were tested, to verify the kinetics of S^{2-} decay. To find the equations that best fit the experimental data, the model of partial order was used,[31] where the reaction rate is made proportional to $[S^{2-}]^n$ and dependent on the applied current, as represented in equations 20 and 21.

$$\text{reaction rate} = k[S^{2-}]^n i^m \quad (20)$$

$$\left[S^{2-}\right]_{(t)}^{1-n} = \left[S^{2-}\right]_{(0)}^{1-n} - k(n-1)\,i^m t \quad (21)$$

where k is the kinetic constant, $[S^{2-}]$ is the S^{2-} concentration in mg L^{-1}, i is the current intensity in A, t is the time in h, and n and m are partial reaction orders. Since in each test both the current intensity and the n value remained constants throughout the electrolysis, equations 20 and 21 can take

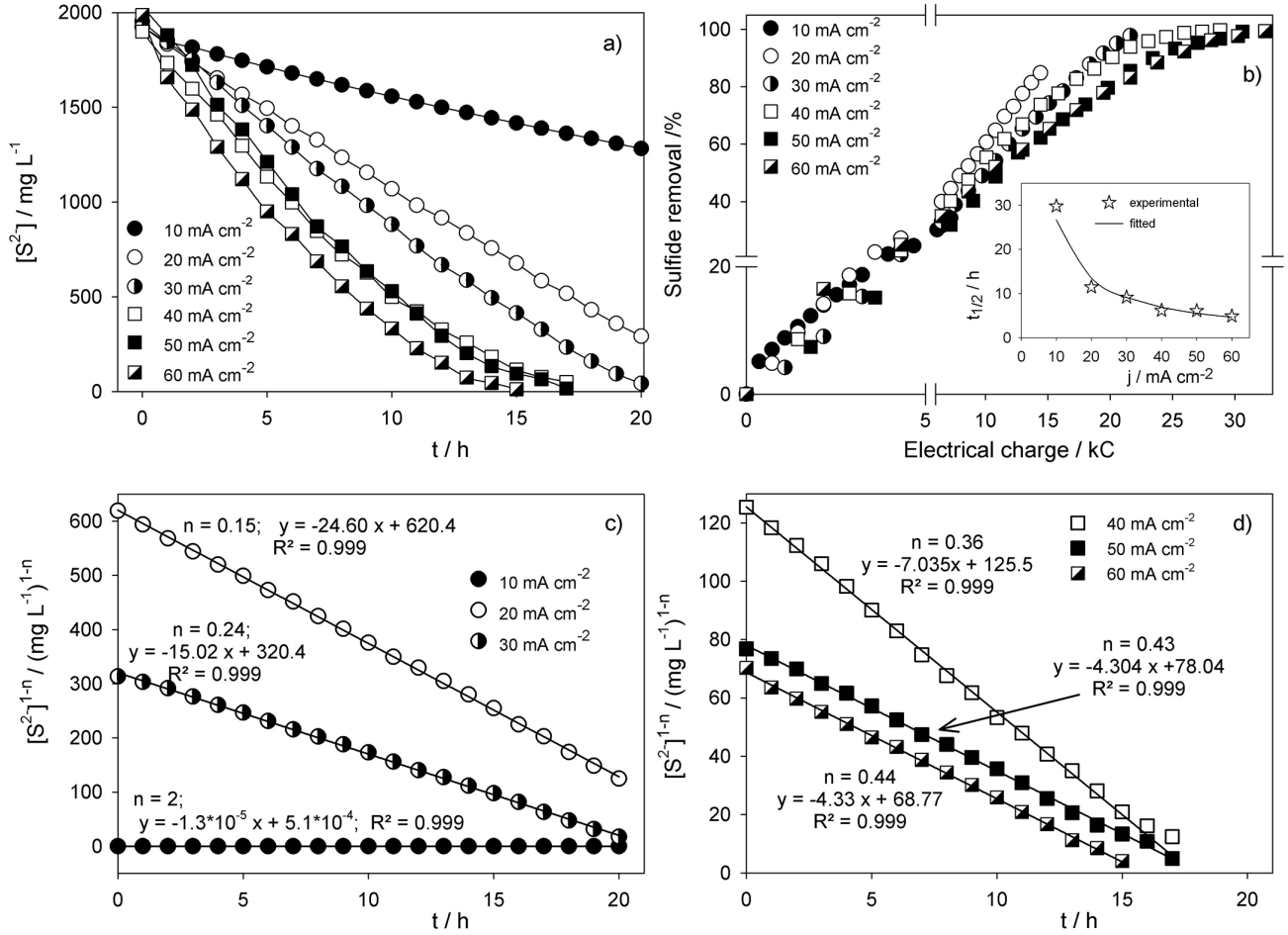

Figure 3. Sulfide removal at different applied current densities: (a) variation of the $[S^{2-}]$ with time; (b) variation of the sulfide removal with the electrical charge delivered; inset of (b) time needed for the removal of 50% S^{2-} initial concentration; (c) and (d) $[S^{2-}]^{1-n}$ experimental data *versus* time and fittings to the experimental data (equation 21) at different applied current densities. $[S^{2-}]_o$= 60 mmol L^{-1}.

the form of equations 22 and 23, respectively, being k' a pseudo kinetic constant.

$$\text{reaction rate} = k'[S^{2-}]^n \quad (22)$$

$$\left[S^{2-}\right]_{(t)}^{1-n} = \left[S^{2-}\right]_{(0)}^{1-n} - k't \quad (23)$$

The analysis of $[S^{2-}]^{1-n}$ *versus* time, at constant current density, were carried out by varying n in steps of 0.01, until the best correlation factor was obtained for each applied current density. For the experiments run with 60 mmol L^{-1} sulfide initial concentration, at different current densities, the optimal n values and the fitted equations are presented in Table 1 and Figures 3c and 3d.

The different orders found for the different applied current densities suggest that the kinetics of the S^{2-} oxidation is strongly influenced by the current density. For 10 mA cm^{-2}, the results showed a second-order reaction related to S^{2-}. This behavior can be explained if it is assumed that the system was on kinetic control and the low flow of electrons gives priority of reactions involving few electrons, i.e., equations 1 and 2. The presence in these reactions of two S^{2-} species as reagent may explain the second order kinetics experimentally observed for the lowest applied current density, when the process is controlled by current and the most probable reactions are those involving few electrons. However, if data for the first 3 h of the assay run at 10 mA cm^{-2} are excluded, a straight line between of $[S^{2-}]$ *versus* time could be adjusted, pointing to a zero order reaction, i.e., reaction rate independent of the $[S^{2-}]$. The increase in current density to the double, 20 mA cm^{-2}, reduces the current control and gives more relevance to the S^{2-} diffusion. A further increase in the current density leads to an increase in the reaction order, showing that the system tends to be controlled by diffusion. A value for the reaction order that is different from an integer is typically indicative of a complex mechanism that, in this case, must be the result of the different extent of several possible reactions, where S^{2-} is consumed; and a competition by the intermediate species for the electric charges (equations 4 and 11 to 13), among others.

Considering the various possibilities for the S^{2-} oxidation, regarding the possible species formed, it was evaluated the behavior of S^{2-} during the oxidation process in relation to the SO_4^{2-} formation for the two extremes situations: a: transfer of 2 electric charges: oxidation of S^{2-} to S, equation 1; b: transfer of 8 electric charges: oxidation of S^{2-} to SO_4^{2-}, equations 10 or 16. Figure 4 presents the theoretical decays in $[S^{2-}]$ if only extremes scenarios a and b were possible, as well as the real scenario. Scenarios a and b were calculated using the respective current intensities and Coulomb's law (equation 24).

$$q = it \quad (24)$$

where q is the electric charge, in C, and t is in s. According to Figures 4a to 4f, the decrease in the S^{2-} concentration showed intermediate behavior between the exclusive formation of elemental sulfur and the direct formation of SO_4^{2-}, i.e., the oxidation of S^{2-} occurs in steps in which the intermediate oxygenated species are formed and oxidized gradually to SO_4^{2-}. If there was a direct oxidation to SO_4^{2-}, the decrease in S^{2-} concentration would be less effective; on the other hand, if there was only oxidation of S^{2-} to elemental sulfur, the decay of the S^{2-} concentration would be dramatically higher. So, the reaction pathway involves the occurrence of the reactions described by equations 2 and 4 to 6, where the sulfur formed on the surface of BDD reacts with the S^{2-} producing S_x^{2-}. In fact, the formation of S_x^{2-} was observed, since the liquid phase presented a yellow color. However, polysulfides produced are consumed, producing SO_4^{2-} as a final step, which explains the loss in the yellow coloration.

Sulfate formation

Regardless of the applied current density, in all assays there was the formation of SO_4^{2-}. However, its formation rate is strongly influenced by the current density, following a linear trendline, as can be seen in Figure 5a for the initial S^{2-} concentration of 60 mmol L^{-1}. The linear equations adjusted to the experimental data up to the fifteenth hour of the assay are presented in Table 2.

The S^{2-} oxidation to SO_4^{2-} can happen either by direct oxidation (equations 10 or 16) or by indirect reactions (equation 15 followed by 13), and the greater the availability of electrons, the higher the sulfate formation rate. To better understand the formation of SO_4^{2-} from the oxidation of S^{2-}, equation 25 was adjusted to the experimental data obtained for the SO_4^{2-} formation rate, being assumed that SO_4^{2-} is

Table 1. Reaction pseudo-orders for the kinetics of the $[S^{2-}]$ decay at different current densities

j / (mA cm^{-2})	10	20	30	40	50	60
Reaction order (n)	2.0	0.15	0.24	0.36	0.43	0.44

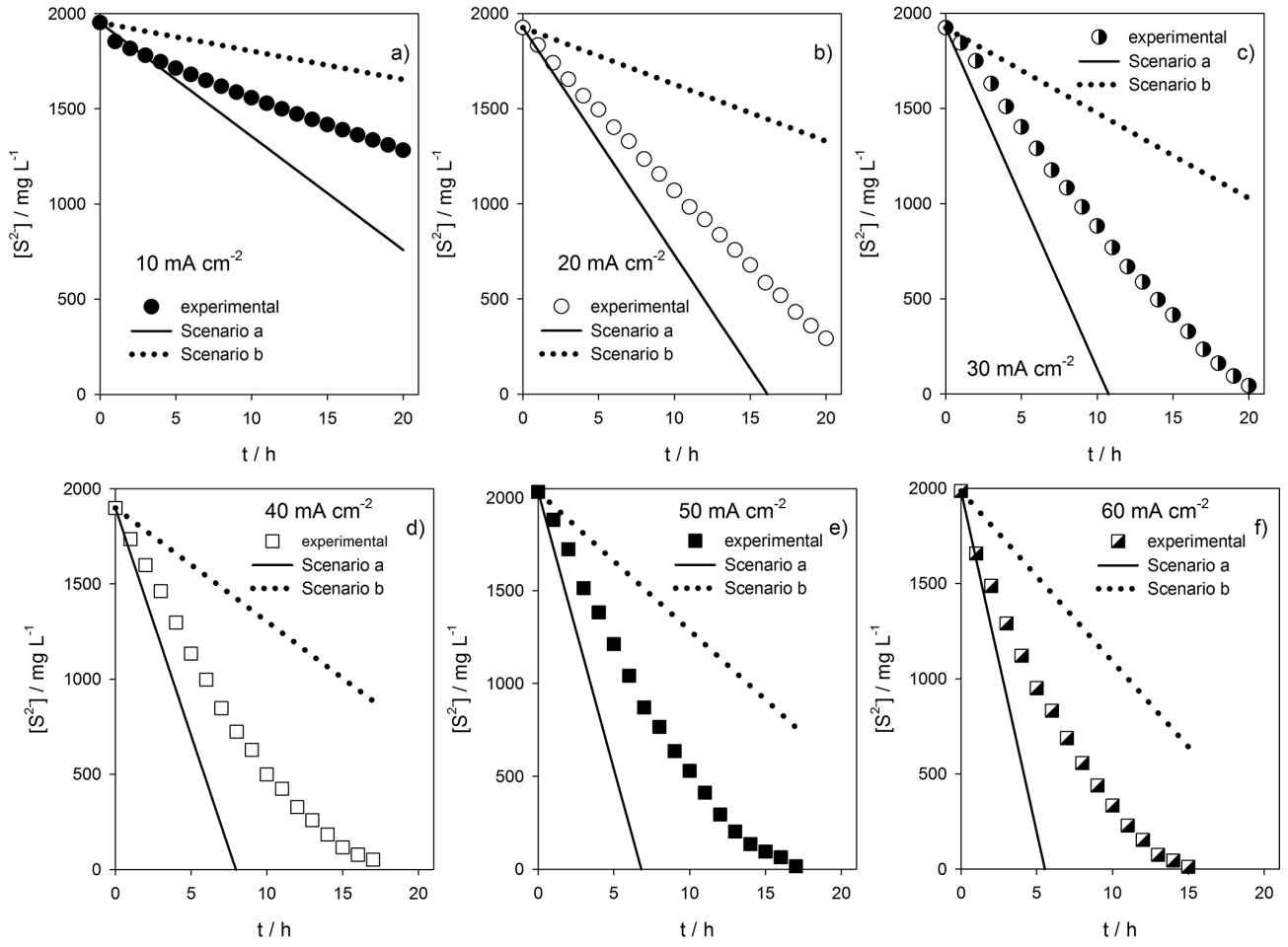

Figure 4. Variation of S^{2-} concentration with time in different scenarios: experimental (symbols); oxidation through equation 1 (scenario a); and oxidation through equations 9 or 15 (scenario b). Applied current densities of (a) 10; (b) 20; (c) 30; (d) 40; (e) 50 and (f) 60 mA cm^{-2}. $[S^{2-}]_o$= 60 mmol L^{-1}.

Table 2. Variation of sulfate concentration, in mg L^{-1}, with time, in h, and kinetic data (equation 25) for the formation of SO_4^{2-} from S^{2-} electro-oxidation, for different applied current densities

j / (mA cm^{-2})	Adjusted equations	R^2	k'' / (mg L^{-1} h^{-1} A^{-1})	m'
10	$[SO_4^{2-}] = 30.47t + 178.6$	0.990	348	1.05
20	$[SO_4^{2-}] = 178.6t + 128.6$	0.993	951	1.00
30	$[SO_4^{2-}] = 264.6t - 146.3$	0.992	905	1.00
40	$[SO_4^{2-}] = 342.5t - 96.94$	0.996	794	1.00
50	$[SO_4^{2-}] = 374.5t + 3.217$	0.998	682	1.00
60	$[SO_4^{2-}] = 400.1t + 74.70$	0.999	667	1.04

k'': kinetic pseudo-constant for the sulfate formation; m': reaction order for current intensity.

obtained from S^{2-} oxidation and neglecting the formed intermediates.

$$\frac{d\left[SO_4^{2-}\right]}{dt} = k'' \left[S^{2-}\right]^{n'} i^{m'} \quad (25)$$

where k'' is a kinetic pseudo-constant for the sulfate formation, n' and m' are the reaction order for $[S^{2-}]$ and for current intensity, respectively. By applying natural logarithm to equation 25 and using the Solver tool from Excel, the values of k'', n' and m' were calculated, using the experimental data for the variation of $[SO_4^{2-}]$ and $[S^{2-}]$ with time. The obtained values are presented in Table 2, except for n' that is equal to zero for all the applied current densities tested, and it can be observed that the sulfate formation is only dependent on the current density. Lower current densities originate lower SO_4^{2-} formation yield due to the current control and to the accumulation of intermediate

species, such as S_2^{2-}, S_3^{2-}, SO_3^{2-}, $S_2O_3^{2-}$, and others. To find out the amount of other sulfur oxidized species, different from SO_4^{2-}, the variation of ($[S^{2-}]_0 - [S^{2-}] - [SO_4^{2-}]$) was plotted against time (Figure 5b), showing that the oxidation of S^{2-} may involve the formation of different species, besides the direct conversion into SO_4^{2-}.

In fact, the oxidation conducted at 10 mA cm^{-2} showed the greatest differences in the mass balances, and persistently, indicating that the direct conversion of S^{2-} into SO_4^{2-} via anodic oxidation tends to present greater difficulties, due to the competition with the intermediate species for the available electrons. For 20 mA cm^{-2}, the mass balance showed that consumption of S^{2-} was also followed by intense formation of intermediate species, with the maximum difference between the expected and the total sulfur formed at 18 h of run. Regarding the results for 30 mA cm^{-2}, the mass balance shows low oxidation to SO_4^{2-} until 7 h. Between 7 and 12 h, the accumulation of intermediates remained approximately constant, indicating an increase in their oxidation rate probably due to the decrease in the $[S^{2-}]$ after the 12 h of assay. Concerning 40 and 50 mA cm^{-2}, the trendlines are similar to the ones obtained with the assays performed at 20 and 30 mA cm^{-2}. This similarity in the intermediate species concentration between applied current densities of 20 and 50 mA cm^{-2} does not necessarily mean that the rate of SO_4^{2-} formation is equal, because $[S^{2-}]$ decay increases with current density and, consequently, if the intermediates concentration remains constant, the SO_4^{2-} formation must be higher for the highest applied current density. The highest current density used in the last test, 60 mA cm^{-2}, showed a slightly different behavior. Apparently, this high current intensity promoted more intense oxidation of S^{2-} in the first hours, i.e., generating appreciable concentrations of intermediate sulfur species. As can be seen in Figure 5b, at 5 h it was achieved the maximum concentration of those species, intensifying the competition between them and S^{2-}. After 5 h run, an enhancement in the oxidation rate of the

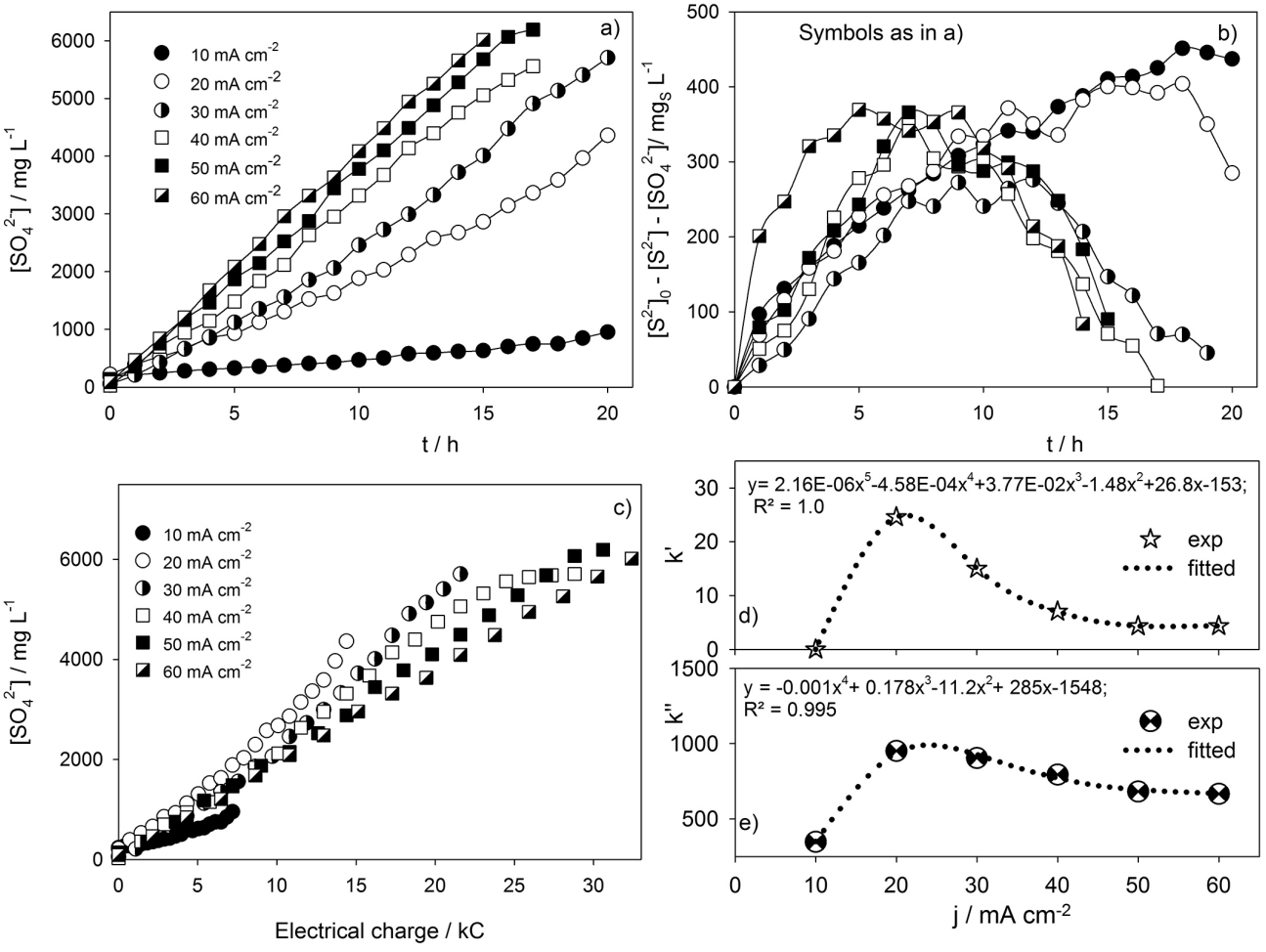

Figure 5. (a) Evolution in time of the SO_4^{2-} formation for different applied current density; (b) evolution in time of the sulfur species other than sulfide or sulfate, for different applied current densities; (c) variation of the sulfate formation with the electrical charge delivered; (d) reaction pseudo-kinetic constants for the electro-oxidation of S^{2-} and (e) for the formation of SO_4^{2-} from S^{2-} electro-oxidation, for the different applied current densities. $[S^{2-}]_o$= 60 mmol L^{-1}.

intermediates species or a reduction on their formation rate is observed. The current efficiency for the formation of sulfate from sulfide oxidation is depicted in Figure 5c, being the lowest efficiency observed for 10 mA cm^{-2}, probably because reactions involving lower number of electrons are favored, leading to low sulfate formation rate. On the other hand, the highest current efficiency regarding sulfate formation is observed for 20 mA cm^{-2}, since this must be the lowest current density that maintains the process in diffusional control, but with low oxygen evolution. For current density higher than 20 mA cm^{-2}, the process is clearly in diffusional control, wasting part of the applied current in oxygen evolution, which increases with applied current.

The influence of the applied current density on the direct formation of sulfate from sulfide can also be visualized in Figures 5d and 5e, where the pseudo-kinetic constants k' and k'', obtained from data presented on Figures 3c and 3d, and Table 2, are plotted against the current density. If data for 10 mA cm^{-2} is excluded, it can be observed that the decay in [S^{2-}] is less influenced by changes in the applied current density than the sulfate formation rate, meaning that an increase in the current density will increase mainly the conversion of the intermediate species to sulfate rather than the oxidation of sulfide to intermediate species. The k' and k'' values for 10 mA cm^{-2} can be explained by the low current intensity that greatly increases the current control.

Conclusion

The obtained results have proved that sulfide can be efficiently converted to sulfate by electrochemical oxidation using a BDD anode and that the process can be used to efficiently remove sulfide from effluents, even when its concentration is high. The following conclusions were also obtained: (*i*) oxidation of S^{2-} to SO_4^{2-} occurs in stages, characterized by the formation of sulfurous intermediate species, oxygenated or not, whose concentration tends to be lower with the increase in the applied current density. (*ii*) The oxidation of S^{2-} does not follow a single pathway, being dependent on the applied current density and presenting order 2 for the lower applied current density, which is compatible with a mechanism involving two S^{2-} ions to give S_2^{2-}. For higher applied current densities, where the current control is less important, the reaction order varies from 0.15 to 0.44 for the applied current densities of 20 and 60 mA cm^{-2}, respectively. (*iii*) The formation of SO_4^{2-} is strongly influenced by the applied current density, probably due to the involvement of hydroxyl radicals, and it is not dependent on the sulfide concentration.

Acknowledgments

The authors are much grateful to Coordenação de Aperfeiçoamento de Pessoal de Ensino Superior, CAPES, for financing the PhD grant (Bolsista da CAPES, Proc. No. BEX 0714/13-5). Authors also want to acknowledge Fundação para a Ciência e a Tecnologia for the project PEst-OE/CTM/UI0195/2014 of the FibEnTech Research Unit.

References

1. Cai, J.; Zheng, P.; *Bioresour. Technol.* **2013**, *128*, 760.
2. Park, K.; Lee, H.; Phelan, S.; Liyanaarachchi, S.; Marleni, N.; Navaratna, D.; Jegatheesan, V.; Shu, L.; *Int. Biodeterior. Biodegrad.* **2014**, *95*, 251.
3. Garcia-de-Lomas, J.; Corzoa, A.; Portillo, M. C.; Gonzalez, J. M.; Andrades, J. A.; Saiz-Jimenez, C.; Garcia-Robledo, E.; *Water Res.* **2007**, *41*, 3121.
4. Haner, J.; Bejan, D.; Bunce, N. J.; *J. Appl. Electrochem.* **2009**, *39*, 1733.
5. Murugananthan, M.; Raju, G.; Prabhakar, S.; *J. Hazard. Mater.* **2004**, *109*, 37.
6. Zhang, L.; Schryver, P.; Gusseme, B.; Muynck, W.; Boon, N.; Verstraete, W.; *Water Res.* **2008**, *42*, 1.
7. Dutta, P. K.; Rabaey, K.; Yuan, Z.; Keller, J.; *Water Res.* **2008**, *42*, 4965.
8. Waterston, K.; Bejan, D.; Bunce, N. J.; *J. Appl. Electrochem.* **2007**, *37*, 367.
9. Rajeshwar, K.; *J. Appl. Electrochem.* **1994**, *24*, 1077.
10. Panizza, M.; Cerisola, G.; *Environ. Sci. Technol.* **2004**, *38*, 5470.
11. Ateya, B. G.; Al-Kharafi, F. M.; Abdallah, R. M.; Al-Azab, A. S.; *J. Appl. Electrochem.* **2005**, *35*, 297.
12. Valensi, G.; Van, J. M.; Pourbaix, M. In *Atlas d'Équilibres Électrochimiques a 25 °C*; Pourbaix, M.; Zubov, N.; Van, J. M., eds.; Gauthier-Villars: Paris, 1963, ch. 4, section 4.19, p. 540.
13. Druschel, G. K.; Hamers, R. J.; Banfield, J. F.; *Geochim. Cosmochim. Acta* **2003**, *67*, 4457.
14. Awe, S. A.; Sundkvist, J. E.; Sandström, Å.; *Miner. Eng.* **2013**, *53*, 39.
15. Greenwood, N. N.; Earnshaw, A.; *Chemistry of the Elements*; Pergamon Press: Oxford, 1984.
16. Zopfi, J.; Ferdelman, T. G.; Fossing, H.; *Geol. Soc. Am., Spec. Pap.* **2004**, *379*, 97.
17. Kleinjan, W. E.; Keizera, A.; Janssen, A. J. H.; *Water Res*. **2005**, *39*, 4093.
18. Ensafi, A. A.; Soleymani, H. A.; Mirmomtaz, E.; *Microchem. J.* **2008**, *89*, 108.
19. Ateya, B. G.; Al-Kharafi, F. M.; *Electrochem. Commun.* **2002**, *4*, 231.
20. Miller, B.; Chen, A.; *Electrochim. Acta* **2005**, *50*, 2203.

21. Pikaar, I.; Rozendal, R. A.; Yuan, Z.; Keller, J.; Rabaey, K.; *Water Res.* **2011a**, *45*, 2281.
22. Pikaar, I.; Rozendal, R. A.; Yuan, Z.; Keller, J.; Rabaey, K.; *Water Res.* **2011b**, *45*, 5381.
23. Panizza, M.; Cerisola, G.; *Chem. Rev.* **2009**, *109*, 6541.
24. Anglada, A.; Urtiaga, A.; Ortiz, I.; *J. Chem. Technol. Biotechnol.* **2009**, *84*, 1747.
25. Szpyrkowicz, L.; Kaul, S. N.; Neti, R. N.; Satyanarayan, S.; *Water Res.* **2005**, *39*, 1601.
26. APHA; *Standard Methods for the Examination of Water and Wastewater*, 21st ed.; American Public Health Association, Washington, 2005.
27. Al-Kharafi, F. M.; Saad, A. Y.; Ateya, B. G.; Ghayad, I. M. C.; *Mod. Appl. Sci.* **2010**, *4*, 2.
28. Hastie, J.; Bejan, D.; Bunce, N. J.; *Can. J. Chem. Eng.* **2011**, *89*, 948.
29. Rysselberghe, P. V.; Gropp, A. H.; *J. Chem. Educ.* **1944**, *21*, 96.
30. Milazzo, G.; Caroli, S.; Sharma, V. K.; *Tables of Standard Electrode Potentials*; Wiley: Chichester, 1978.
31. Li, S.; Bejan, D.; McDowell, M. S.; Bunce, N. J.; *J. Appl. Electrochem.* **2008**, *38*, 151.

Submitted: March 9, 2016
Published online: June 30, 2016